these computational difficulties. Again, the terms in the series are large and alternate in sign. Note that while the Barbiere series is a power series in inverse powers of $\beta > 1$, this does not really help because β approaches unity as N becomes large.

The van der Maas [3] solution (3) is a definite improvement. All terms in the series now have the same sign, and the solution is a power series in ascending powers of $\alpha < 1$ where α now approaches zero as N becomes large. However, for large N, even this solution involves ratios of factorials of large numbers. The computation of these factorials is often beyond the capabilities of the average "scientific calculator" and even of many "desk-top computers." It is possible to circumvent this problem, but then the computation of each term of the series becomes tedious and the amount of computational labor again becomes prohibitive.

van der Maas [3] and others [4], [5] have also considered a variety of approximate solutions. These are not discussed here. The "nested product" (NP) formulation described in this paper provides an exact solution for the array current distribution.

II. SOLUTION VIA THE "NESTED-PRODUCT" ALGORITHM

Two versions of the van der Maas solution appear in (3). The first version is the one that is obtained naturally when [3, eq. (8)] is simply reordered to conform to the numbering conventions of Fig. 1. A further reordering is then introduced to put the solution into a form consistent with that employed in (4) to define the nested-product polynomial NP(n, f_m, α), a finite polynomial of degree $(n-1)$:

$$\begin{aligned}\mathrm{NP}(n, f_m, \alpha) &\equiv \sum_{m=1}^{n} \alpha^{n-m} \cdot \prod_{j=m}^{n} f_j; \qquad f_n \equiv 1 \\ &= \alpha^{n-1} \prod_{j=1}^{n-1} f_j + \alpha^{n-2} \prod_{j=2}^{n-1} f_j + \cdots \\ &\quad + \alpha f_{n-1} + 1 \\ &= \{[\cdots(\cdots(f_1\alpha + 1)f_2\alpha + \cdots + 1) \\ &\quad \cdot f_m\alpha + \cdots + 1]f_{n-1}\alpha + 1\}, \end{aligned} \tag{4}$$

where

$$f_m \equiv \left(\prod_{j=m}^{n-1} f_j \Big/ \prod_{j=m+1}^{n-1} f_j \right) \qquad m = 1, 2, 3 \cdots n-1.$$

The essential features of this definition are that the coefficients of the higher order powers of α contain all the factors which appear in the coefficients of all of the subsequent lower order terms and that $f_n = 1$. Thus, to identify the second of the equations in (3) as a set of nested-product polynomials the common factor $(n-1)!$ must remain within the summation symbol, because it is the ratio $[(n-1)!/(m-1)!]$ that satisfies this requirement, not $(m-1)!$ alone.

A comparison of the second of the equations in (3) with the definition in (4) now permits us to write the solution for the array excitation coefficients as

$$I_{N-n} = (M-1)\alpha \cdot \mathrm{NP}\ (n, f_m, \alpha)$$

$$f_m = \frac{m(M-1-2n+m)}{(n-m)\cdot(n+1-m)}.$$

The nested product polynomials NP(n, f_m, α) are evaluated via a sequence of computations equivalent to the following FORTRAN DO loop:

```
ALPHA   = ···
NP      = 1.0
DO ···  m = 1, n - 1
F(m)    = m*(M - 1 - 2*n + m)/((n - m)*(n + 1 - m))
NP      = NP*ALPHA*F(m) + 1.0
CONTINUE
```

This computation is readily accomplished, even for very large arrays, with a typical programmable scientific calculator or desk-top computer.

REFERENCES

[1] C. L. Dolph, "A current distribution for broadside arrays which optimizes the relationship between beamwidth and side lobe level," *Proc. IRE*, vol. 34, pp. 335–348, June 1946.

[2] D. Barbiere, "A method for calculating the current distribution of Tschebyscheff arrays," *Proc. IRE*, vol. 40, pp. 78–82, January 1952.

[3] C. J. van der Maas, "A simplified calculation for Dolph–Tchebycheff arrays," *J. Appl. Phys.*, vol. 25, no. 1, pp. 121–124, Jan. 1954.

[4] R. J. Stegen, "Excitation coefficients and beamwidths of Tschebyscheff arrays," *Proc. IRE*, vol. 41, no. 11, pp. 1671–1674, Nov. 1953.

[5] A. N. Nuttal, "Generation of Dolph–Chebyshev weights via a fast Fourier transform," *Proc. IEEE*, vol. 62, pp. 1396, Oct. 1974.

Some Important Geometrical Features of Conic-Section-Generated Offset Reflector Antennas

V. JAMNEJAD-DAILAMI, MEMBER, IEEE, AND YAHYA RAHMAT-SAMII, SENIOR MEMBER, IEEE*

***Abstract*—Geometrical characteristics of conic-section-generated offset reflectors are studied in a unified fashion. Some unique geometrical features of the reflector rim constructed from the intersection of the reflector surface and a cone or cylinder are explored in detail. It is found that the intersection curve (rim) of the rotationally generated conic-section reflector surface and a circular cone with its tip at the focal point is always a planar curve and has a circular projection on the focal plane only for the offset parabolic reflector. Furthermore, in this case, the line going through the center**

Manuscript received February 6, 1980; revised July 7, 1980. This paper presents the results of one phase of research carried out at the Jet Propulsion Laboratory, California Institute of Technology, under Contract No. NAS 7-100, sponsored by NASA.

The authors are with the Jet Propulsion Laboratory, California Institute of Technology, Pasadena, CA 91103.

* The order of listing of the authors is arbitrary.

0018-926X/80/1100-0952$00.75 © 1980 IEEE

of the circle, parallel to the focal axis, and the central axis of the cone do not intersect the reflector surface at the same point. Numerical results are presented to demonstrate some unique features of offset parabolic reflectors.

I. INTRODUCTION

Both single and dual offset reflector antennas are finding considerable application in the design of low-sidelobe multibeam antenna systems [1]–[4]. Due to their very unique optical focusing characteristics, surfaces generated from conic sections are most commonly used in practice. Typically, these surfaces are constructed as a result of a translation or rotation of the conic sections. In this work, rotationally generated reflector surfaces are studied. Offset reflectors are carved-out portions of the surface, resulting from its intersection with a cylinder or cone. The cylinder has its axis parallel to the rotation axis of the parent reflector surface, and the cone has its tip at one of the foci of the reflector.

In this work, geometrical characteristics of the conic-section offset reflectors are studied in a unified fashion. In particular, some of the important geometrical features of the reflector rim are explored in detail, since this information is important in calculating the performance of the antenna. It is shown that the intersection curve (rim) of the rotationally generated conic-section reflector surface with a circular cone, which has its tip at the focal point, is always a planar curve and has a circular projection on the focal plane only in the case of the offset parabolic reflector. Furthermore, it is shown that, in this case, the ray along the cone axis reflects along a line other than the central axis of the reflected circular cylindrical bundle of rays. This fact has applications in the design of the pointing direction of the feed with respect to the reflector surface. Analytical expressions and numerical results are presented to assist the reader in designing geometrical configurations of the offset reflector antennas.

II. CONIC SECTIONS

Conic sections are basically second-degree planar curves which can be generated in a variety of ways, including the intersection of a circular cone with planar surfaces. Referring to Fig. 1, with z as the abscissa and y as the ordinate of a plane Cartesian coordinate system, one can express the equation of a conic section in the following general form:

$$\frac{(z-c)^2}{(f+c)^2}+\frac{y^2}{(f+c)^2-c^2}=1. \tag{2.1}$$

In the polar coordinates this equation is written as

$$\rho=\frac{f+2c}{f+(1-\cos\phi)c}f, \tag{2.2}$$

where in both of the above equations the parameters have the following definitions: f is the focal length (distance from a focus to the nearest apex) having a positive or zero value and $2c=\overrightarrow{F_1F_2}\cdot\hat{z}$ is the distance between the two foci having an algebraic value. It is positive if F_2 is to the right of F_1 and negative otherwise. ($\hat{z}$ is a unit vector along the positive z direction.)

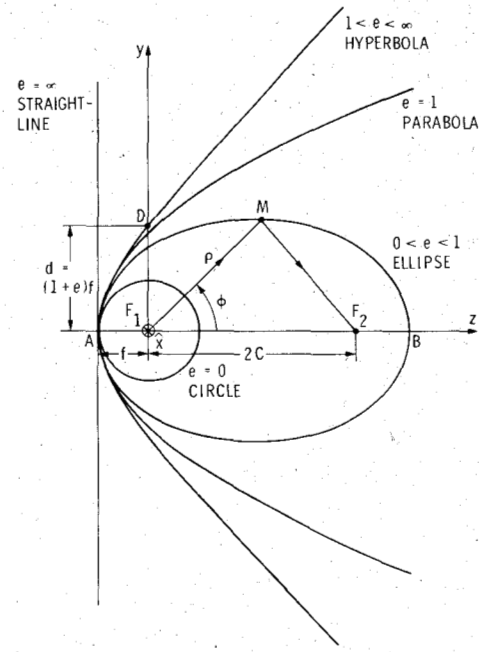

Fig. 1. Geometrical configuration of conic sections as a function of eccentricity e, for fixed focal length f.

One of the common properties of the conic sections is that either the sum or difference of distances from any point on the curve to the focal points is constant. Another manifestation of this property from the geometrical optics viewpoint is that any ray passing through one focus and crossing the curve at a given point is reflected along the line connecting the crossing point to the second focus, since incident and reflected rays make equal angles with respect to the normal at the crossing point.

Eccentricity e is defined as

$$e=\frac{c}{c+f}=\frac{1}{1+f/c}, \tag{2.3}$$

which is always a positive number. This parameter is a measure of the off-centeredness of the focal points for a given focal length. Note that the center is located at the midpoint of the foci. Thus when the foci are at the center (circle) the eccentricity is zero, and when they are infinitely apart it is unity (parabola) and so on. In terms of this new parameter, (2.1) and (2.2) can be rewritten as

$$\frac{\left(z-\frac{e}{1-e}f\right)^2}{\frac{1}{(1-e)^2}f^2}+\frac{y^2}{\frac{1-e^2}{(1-e)^2}f^2}=1 \tag{2.4}$$

and

$$\rho=\frac{1+e}{1-e\cos\phi}f. \tag{2.5}$$

In order to better appreciate the characteristics of these conic-section curves, the cases in Table I are outlined. For the sake of comparison, all the conic sections with one com-

TABLE I

Foci Separation/2	Eccentricity	Equation	Type
$c = 0$	$e = 0$	$\frac{z^2}{f^2} + \frac{y^2}{f^2} = 1$	circle
$0 < c < \infty$	$0 < e < 1$	(2.4)	ellipse
$c = \infty$	$e = 1$	$(z + f) - \frac{1}{4f} y^2 = 0$	parabola
$-\infty < c < -2f$	$1 < e < \infty$	(2.4)	hyperbola
$c = -f$	$e = \infty$	$z + f = 0$	straight line

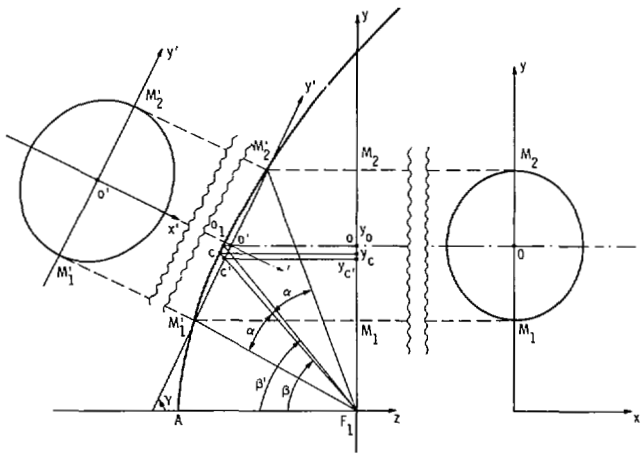

Fig. 2. Geometry of an offset reflector obtained from intersection of a surface generated by rotation of a conic section around its focal axis, and a circular cone.

mon focal point and identical focal length are superimposed in Fig. 2. As eccentricity e increases, the curves broaden, i.e., $F_1D(= d)$, and R, the radius of curvature at the apex A, increase accordingly, since it can be shown that

$$R = d = (1 + e)f. \tag{2.6}$$

III. REFLECTOR SURFACES

Reflector surfaces are commonly generated either by the translation of a conic section along the x axis or by its rotation about the focal axis z, as in Fig. 1. In this study the rotationally generated surfaces are considered.

An offset reflector can be constructed by carving out a portion of the rotationally symmetric reflector. This is typically achieved by either intersecting the reflector with a circular or elliptical cylinder with its axis parallel to the reflector axis, or by intersecting the reflector with a circular or elliptical cone with its tip at the focal point. This section studies the geometrical characteristics of the reflector rim thus obtained.

A. Intersection with a Circular Cone

The cone of rays emanating from a source located at the focal point F_1 intersects the reflector surface as shown in Fig. 3. The equation of the reflector surface, produced by the

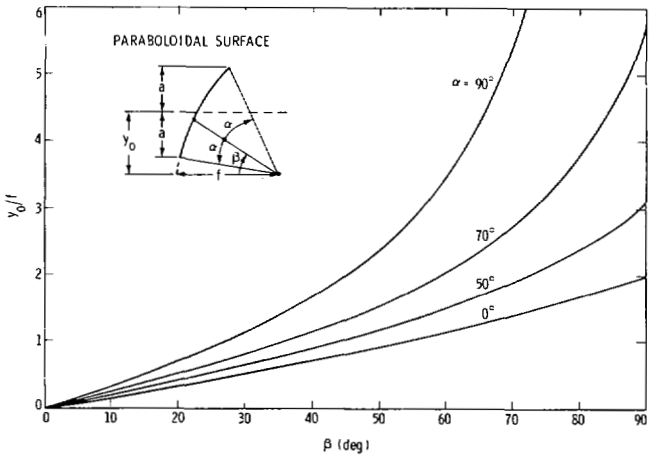

Fig. 3. Normalized offset height y_o/f versus angle β for various values of angle α (see (3.16)).

revolution of a conic section about the z axis, is obtained by simply replacing y^2 by $x^2 + y^2$ in (2.4) to arrive at

$$\frac{\left(z - \frac{e}{1-e} f\right)^2}{\frac{1}{(1-e)^2} f^2} + \frac{x^2 + y^2}{\frac{1-e^2}{(1-e)^2} f^2} = 1. \tag{3.1}$$

The equation of a cone whose axis lies in the y–z plane, making an angle β with the negative z axis and having a half-angle α, as shown in Fig. 3, is

$$(x^2 + y^2 + z^2) \cos^2 \alpha = (y \sin \beta - z \cos \beta)^2. \tag{3.2}$$

The equation of the intersection curve of the surface of revolution and the cone is the solution of (3.1) and (3.2). The elimination of the x variable from these equations leads to the projection of the intersection curve on the y–z plane, and the final result is

$$y \sin \beta - z \cos \beta = \pm [ez + (1 + e)f] \cos \alpha, \tag{3.3}$$

where the positive sign must be chosen for the intersection in the second quadrant of the y–z plane. Thus

$$y = \frac{\cos \beta + e \cos \alpha}{\sin \beta} z + \frac{(1 + e) \cos \alpha}{\sin \beta} f \tag{3.4}$$

is the equation of the projection of the intersection on the y–z plane. Clearly this projection is a *straight* line, indicating that the intersection curve (rim) lies in a *plane* perpendicular to the y–z plane. In other words, it is shown that the intersection of a reflector surface, generated from the rotation of a conic section about its focal axis, and a circular cone, with its tip on a focal point of the reflector surface, is always a *planar curve*. In fact, it will be shortly demonstrated that this curve is an ellipse.

Eliminating the variable z between (3.1) or (3.2) and (3.4), one obtains the equation of the projection of the intersection curve (rim) on the x–y plane. This elimination process is rather

lengthy, and the final result is

$$\frac{x^2}{a^2}+\frac{(y-y_0)^2}{b^2}=1, \tag{3.5}$$

in which

$$y_0=\frac{(1+e)(e\cos\beta+\cos\alpha)\sin\beta}{(1-e^2)\sin^2\beta+(\cos\beta+e\cos\alpha)^2}f$$

$$a^2=\frac{(1+e)^2\sin^2\alpha}{(1-e^2)\sin^2\beta+(\cos\beta+e\cos\alpha)^2}f^2$$

$$b^2=\frac{(1+e)^2(\cos\beta+e\cos\alpha)^2\sin^2\alpha}{[(1-e^2)\sin^2\beta+(\cos\beta+e\cos\alpha)^2]^2}f^2. \tag{3.6}$$

It is now an easy matter to determine the equation of the intersection curve (rim) in the plane of intersection. This is done by designating the x'-y' plane as the intersection plane, as shown in Fig. 2, and choosing $0'$ as the origin of this coordinate system, which allows one to introduce the following changes of variables:

$$x=x'$$

$$y=y'\sin\gamma+y_0 \tag{3.7}$$

where $\tan\gamma$ is the slope of the line defined by (3.4), namely,

$$\tan\gamma=\frac{\cos\beta+e\cos\alpha}{\sin\beta}. \tag{3.8}$$

Substituting (3.7) into (3.5) and simplifying the result, one finally arrives at

$$\frac{x'^2}{a'^2}+\frac{y'^2}{b'^2}=1, \tag{3.9}$$

where

$$a'^2=a^2$$

$$b'^2=\frac{(1+e)^2[\sin^2\beta+(\cos\beta+e\cos\alpha)^2]\sin^2\alpha}{[(1-e^2)\sin^2\beta+(\cos\beta+e\cos\alpha)^2]^2}f^2, \tag{3.10}$$

in which a is given in (3.6).

It is of some interest to note that the point of intersection of the cone axis with the intersection plane, i.e., point c', does not coincide with the center of the intersection curve, i.e., point $0'$ (Fig. 2). This is easily demonstrated by calculating the ordinate of the point c', in the y-z plane with the final result of

$$y_{c'}=\frac{(1+e)\cos\alpha\sin\beta}{1+e\cos\alpha\cos\beta}f, \tag{3.11}$$

which is clearly different from $y_{0'}=y_0$ given in (3.6). Neither do the points c (intersection of the cone axis and the reflector surface) and 0_1 (intersection of the line $0'0$, and the reflector surface) coincide. One can show that

$$y_c=y_0|_{\alpha=0}=\frac{(1+e)\sin\beta}{(1+e\cos\beta)}f, \tag{3.12}$$

which is different from $y_{0_1}=y_0$.

1) *Special cases:* The equation of the intersection curve (rim) in the x'-y' plane and its projection on the x-y plane as given by (3.9) and (3.5), respectively, and also the ordinate of some points of interest as given in (3.12), (3.11), and (3.6), are simplified in the following cases.

a) For a spherical surface ($e=0$)

$$a^2=f^2\sin^2\alpha,\qquad a'^2=a^2$$

$$b^2=a^2\cos^2\beta,\qquad b'^2=a^2 \tag{3.13}$$

and

$$y_0=f\sin\beta\cos\alpha$$

$$y_c'=y_0$$

$$y_c=f\sin\beta. \tag{3.14}$$

In this case the intersection curve (rim) is a *circle* and its projection on the x-y plane is an *ellipse* with its minor axis along the y axis.

b) For a paraboloidal surface ($e=1$)

$$a^2=\frac{4\sin^2\alpha}{(\cos\beta+\cos\alpha)^2}f^2,\quad a'^2=a^2$$

$$b^2=a^2,\qquad b'^2=a^2\left[1+\frac{\sin^2\beta}{(\cos\beta+\cos\alpha)^2}\right] \tag{3.15}$$

and

$$y_0=\frac{2\sin\beta}{\cos\beta+\cos\alpha}f$$

$$y_c=\frac{2\sin\beta}{1+\cos\beta}f$$

$$y_{c'}=\frac{2\sin\beta\cos\alpha}{1+\cos\alpha\cos\beta}f. \tag{3.16}$$

In this case the intersection curve (rim) is an *ellipse* with its major axis along the y axis while its projection on the x-y plane reduces to a *circle*. Figs. 3 and 4 show plots of y_0/f and a/f with respect to β for various values of α using (3.15) and (3.16). It is also of interest, in this case, to determine the relationship between the angles β and β' as shown in Fig. 2. After some manipulations one arrives at

$$\tan\beta'=\frac{1}{1-\dfrac{\sin^2\alpha}{2(\cos^2\beta+\cos\beta\cos\alpha)}}\tan\beta. \tag{3.17}$$

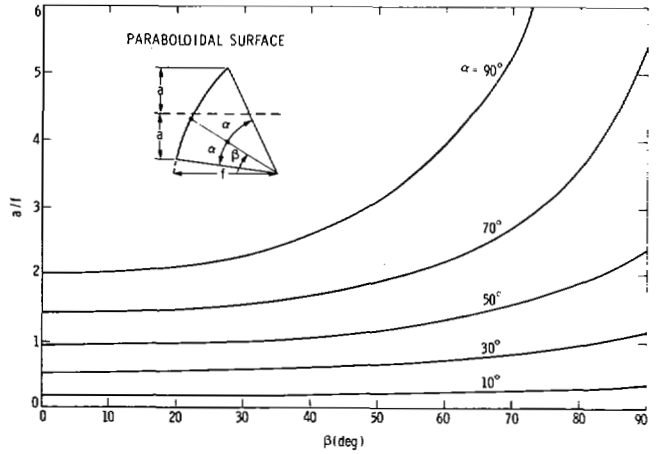

Fig. 4. Normalized radius of projected aperture a/f versus angle β for various values of angle α (see (3.15)).

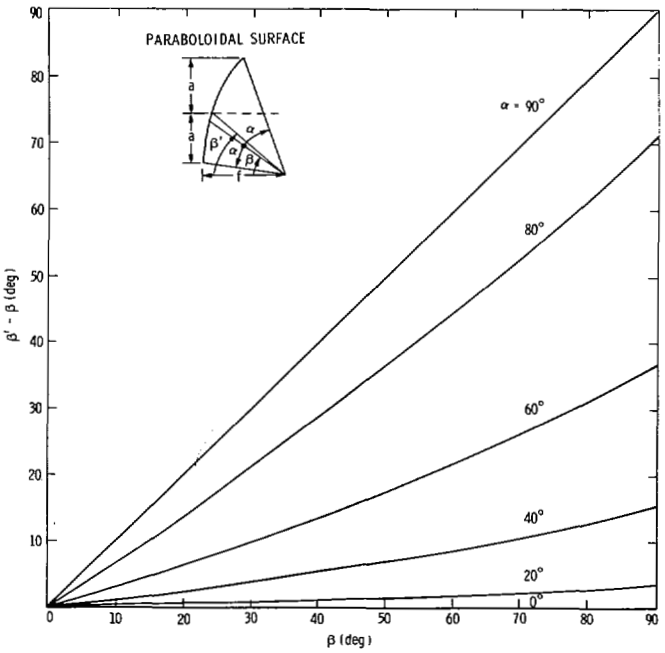

Fig. 5. Difference angle $\beta'-\beta$ versus angle β for various values of α (see (3.17)).

Fig. 5 plots $\beta-\beta'$ versus β for various values of α. Customarily, the feed is directed in the β (see, e.g., [2]) or β' (see, e.g., [3]) direction.

A set of typical far-field patterns with the feed directed in the β and β' directions is shown in Figs. 6 and 7. As seen from these figures, the pattern in the plane of symmetry of the system (Fig. 6) shows some improvement for the feed directed along the β' as opposed to the β direction. In fact, it can be shown that the optimum pattern in the plane of symmetry is achieved for an angle slightly larger than β'. However, in the perpendicular plane (Fig. 7) the differences in the patterns for the two directions are less pronounced and point to slightly better patterns (both copolar and cross polar) for the feed in the β direction. Notice that for the reflector considered here ($\beta = 45°$, $\alpha = 45°$) the difference between angles β and β' is very significant ($\beta'-\beta = 8.13°$), but in most practical cases (smaller β and α) β and β' are very close and the change of feed direction from β to β' has minimal

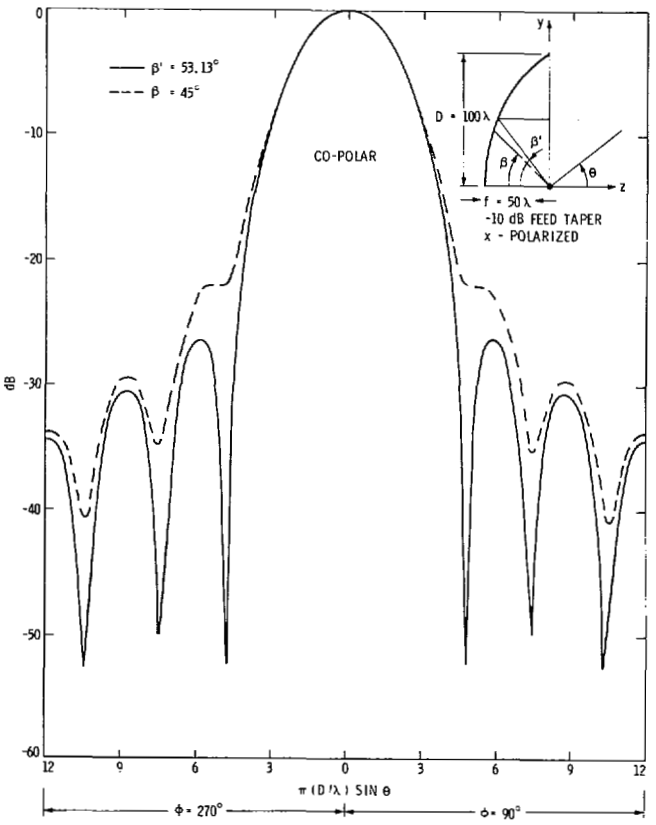

Fig. 6. Far-field patterns in plane of symmetry of antenna system for feed directed along β and β' directions.

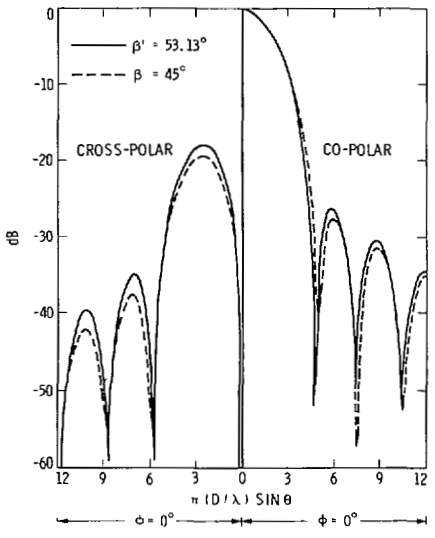

Fig. 7. Copolar and cross-polar components of far-field patterns in plane perpendicular to plane of symmetry of antenna system for feed directed along β and β' directions.

effect on the patterns. In general, the choice of the optimum feed direction should be considered on a case by case basis, although the β' direction seems to produce a better overall antenna pattern.

c) For a plane surface ($e = \infty$)

$$a^2 = \frac{\sin^2 \alpha}{\cos^2 \alpha - \sin^2 \beta} f^2, \qquad a'^2 = a^2$$

$$b^2 = \frac{\cos^2 \alpha}{\cos^2 \alpha - \sin^2 \beta} a^2, \qquad b'^2 = b^2 \tag{3.18}$$

and

$$y_0 = \frac{\cos \beta \sin \beta}{\cos^2 \alpha - \sin^2 \beta} f$$

$$y_c = f \tan \beta$$

$$y_{c'} = y_c. \tag{3.19}$$

It is obvious that in this case the intersection curve (rim) and its projection on the x–y plane are the same and display an *ellipse* elongated in the y direction.

As a concluding remark for this section one can say that, starting from zero eccentricity $e = 0$ (a sphere) where the intersection curve (rim) is a circle, as eccentricity increases the rim curve becomes more oblong in the y' direction. Upon projection onto the x–y plane, however, the curve becomes contracted in the y direction to the extent that for $e = 1$ (a paraboloid) the projected curve becomes a circle. For values of $e < 1$ (an ellipsoid) the projected curve has its minor axis in the y direction, while for values of $e > 1$ (a hyperboloid) it has its major axis in that direction.

B. Intersection with a Circular Cylinder

The equation of a circular cylinder with its axis in the plane y–z and parallel to the z axis is given as

$$x^2 + (y - y_0)^2 = R^2, \tag{3.20}$$

where y_0 and R are the offset height and the radius of the cylinder, respectively. The intersection of this cylinder with the reflector surface can be found from (3.20) and (3.1). The projection of the intersection curve (rim) on the y–z plane is found by eliminating x between these two equations with the final result of

$$(1 - e^2)z^2 - 2e(1 + e)fz + 2yy_0 = (1 + e)^2 f^2 + y_0{}^2 - R^2. \tag{3.21}$$

The above equation, in general, describes a parabola. It is therefore concluded that the rim lies on a *parabolic cylinder* and is *not* a plane curve. However, in the special case of $e = 1$ (paraboloid surface) the curve given by (3.21) is a line, which indicates that the rim is planar and, being the intersection of a circular cylinder and a plane, is indeed an ellipse.

REFERENCES

[1] A. W. Love, *Reflector Antennas*. New York: IEEE Press, 1978.
[2] A. W. Rudge and N. A. Adatia, "Offset-parabolic-reflector antennas: A review," *Proc. IEEE*, vol. 66, pp. 1592–1618, 1978.
[3] R. Mittra, Y. Rahmat-Samii, V. Galindo-Israel, and R. Norman, "An efficient technique for the computation of vector secondary patterns of offset paraboloid reflectors," *IEEE Trans. Antennas Propagat.*, vol. AP-27, pp. 294–304, May 1979.
[4] S. W. Lee, P. Cramer, Jr., K. Woo, and Y. Rahmat-Samii, "Diffraction by an arbitrary subreflector: GTD solution," *IEEE Trans. Antennas Propagat.*, vol. AP-27, pp. 305–316, May 1979.